Journal of Alloys and Compounds 509 (2011) 5551–5554

Contents lists available at ScienceDirect

Journal of Alloys and Compounds

journal homepage: www.elsevier.com/locate/jallcom

Nanocrystalline p-type-cuprous oxide thin films by room temperature chemical bath deposition method

P.B. Ahirrao[a], B.R. Sankapal[b], R.S. Patil[c,*]

[a] Department of Physics, S.V.S.'s Arts and Science College, Dondaicha 425408, India
[b] Thin Film and Nanoscience Laboratory, Department of Physics, North Maharashtra University, Jalgaon 425001, India
[c] Department of Physics, P.S.G.V.P. Mandal's Arts, Commerce and Science College, Shahada 425409, India

ARTICLE INFO

Article history:
Received 27 August 2010
Received in revised form 27 January 2011
Accepted 2 February 2011
Available online 23 February 2011

Keywords:
Cuprous oxide
Nanocrystalline thin films
Chemical method
XRD
SEM
Band gap
Room temperature synthesis

ABSTRACT

Nanocrystalline cuprous oxide (Cu_2O) thin films were synthesized on amorphous glass substrate by using simple room temperature chemical route namely, chemical bath deposition (CBD) method. The deposition kinetics played important role to get good quality nanocrystalline films with uniform thickness. The structural, surface morphological, optical and electrical properties of the films were investigated. Crystallization and growth processes obtained micro-spherical shaped grains of Cu_2O due to agglomeration of smaller nanoparticles. An optical and electrical characterization was performed to study the optical band gap and type of electrical conductivity of the film.

1. Introduction

Cuprous oxide (Cu_2O) belongs to I–VI compound semiconductor material which has been studied for several reasons such as: the natural abundance of starting material (Cu); the easiness of production by Cu oxidation; their non-toxic nature and the reasonably good electrical and optical properties. Cu_2O thin film is a colored film ranging from yellow to red-brown with tailored band gaps depending upon the particle size due to size quantization. Cu_2O thin film nanostructures have attracted significant attention as it is one of the first known p-type direct bandgap semiconductor with an optical bulk bandgap of 2.17 eV [1]. The growing interest in Cu_2O nanostructures is due to its potential photovoltaic material which is with lower cost, nontoxicity and can be prepared in large scale applications [2–4]. The crystal structure of Cu_2O is cubic and is a promising material for solar cell applications [5].

Cuprous oxide can be prepared by many techniques such as, the anodic oxidation of copper through a simple electrolysis process [6], the thermal oxidation method [7], spray pyrolysis [8], reactive magnetron sputtering [9], r.f. magnetron sputtering [10], reactive evaporation [11], sol–gel method [12], electro-deposition [13,14] and chemical methods [15,16]. Many of these methods are expensive; require a high temperature and a high vacuum environment.

Till today, no attempt has been made to synthesize Cu_2O films by simple chemical bath deposition method at room temperature. The choice of this technique centers largely on the fact that it possesses a number of advantages over conventional thin film deposition methods, such as low cost, room temperature, and easy coating of large surfaces. These technologies are based on the controlled release of the metal ions. Hence, aim of this work is focused to prepare and characterize nanocrystalline Cu_2O thin films on to amorphous glass substrate by using simple and low cost chemical bath deposition method.

2. Experimental details

For the deposition of Cu_2O thin film, all the reagents used were of analytical grade (Merck chemicals) and used as supplied without any purification. Copper nitrate [$Cu(NO_3)_2{\cdot}3H_2O$], hydrazin-hydrate [H_6N_2O] and triethanolamine (TEA) were used for the deposition of cuprous oxides (Cu_2O) thin films in an aqueous medium. Double distilled water was used throughout the experiment.

Substrate cleaning plays an important role in the deposition of thin films in order to get better nucleation sites at the substrate surface. Corning glass slides of dimensions, 25 mm × 75 mm × 1 mm were used as substrates. Initially, the substrate were washed with double distilled water (DDW), boiled in chromic acid for 2 h and kept in it for 12 h. Again, the substrates were washed with detergent (soap solution), rinsed in acetone and finally ultrasonically cleaned with DDW before deposition of thin film.

* Corresponding author. Tel.: +91 2565 224250.
E-mail address: rspatil_shahada@yahoo.co.in (R.S. Patil).

0925-8388/$ – see front matter © 2011 Elsevier B.V. All rights reserved.
doi:10.1016/j.jallcom.2011.02.016

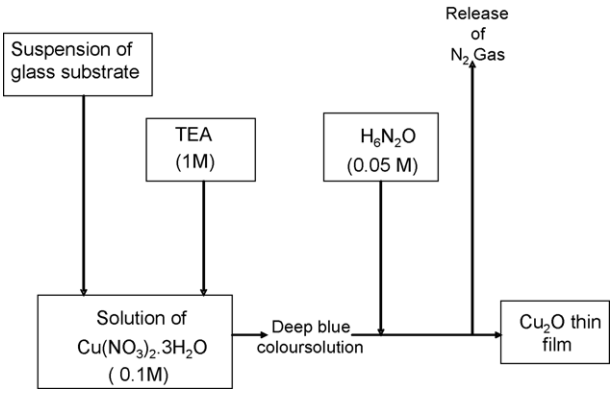

Fig. 1. Flow chart of as-deposited Cu_2O thin film.

Chemical Bath Deposition (CBD) method was used to deposit Cu_2O thin films onto amorphous glass substrate at room temperature. Deposition of thin films of Cu_2O involves 0.1 ML^{-1} copper nitrate, 0.05 ML^{-1} hydrazin-hydrate with 1 ML^{-1} triethanolamine (TEA) as a complexing agent. Taking the 20 ml solution of copper nitrate in a 50 ml beaker, the glass substrate was suspended vertically in the solution with the aid of a beaker cover. The addition of 1 ML^{-1} TEA to copper nitrate solution resulted in a deep blue solution. The further addition of hydrazin-hydrate to the solution resulted in a hissing sound indicating the release of nitrogen gas and a rapid change in colour, first to light blue and then to light yellow, reddish brown, and, finally blue. The optimum growth period was 5 h. The film deposited was pure yellow in colour.

3. Characterizations

The crystallographic orientation as well as structure of the deposited films were studied using X-ray diffractometer (Model Bruker D8 advance AXS) with scanning angles in the range 20–80° using CuK_α radiation ($\lambda = 1.5406$ Å). Scanning electron microscopy (SEM) images were recorded by JOEL, JSM 6360A unit to study the surface morphology of the deposited films. To study the local composition of the deposited films Energy dispersive X-ray analysis (EDAX) couples with SEM unit was used. The optical absorption spectrums of the films were recorded using an UV-Vis-NIR Shimadzu spectrophotometer. The two point probe method was used for electrical resistivity measurements. Thermo e.m.f. measurement unit was used to confirm the p-type electrical conductivity of the film.

4. Results and discussions

During initial deposition process, copper nitrate forms a strong complex with TEA and solution gets saturated, the ionic product is equal to the solubility product. As time passes, strength of complex between copper nitrate and TEA decreases with slow release of copper ions. As the ionic product of the solution (IP) exceeds the solubility product (SP), copper ions gets reacted with the oxygen ions which leads to film deposition [17]. This is the point at which the yellow component of the solution has either been deposited on the substrate or the side of the beaker or has formed sediment leaving a light blue solution.

The flow chart summarizes the formation of Cu_2O which is shown in Fig. 1. The reaction mechanism for Cu_2O thin film deposition is proposed as follows:

$$Cu(NO_3)_2 + TEA \leftrightarrow [Cu(TEA)]^{2+} + 2NO^-_3 \quad (1)$$

$$[Cu(TEA)]^{2+} \leftrightarrow Cu^{2+} + TEA \quad (2)$$

$$H_6N_2O + 2NO^-_3 + 6e^- \leftrightarrow 2H_2O + 2N_2 + 4O^{2-} \quad (3)$$

$$8Cu^{2+} + 4O^{2-} + 8e^- \leftrightarrow 4Cu_2O \downarrow \quad (4)$$

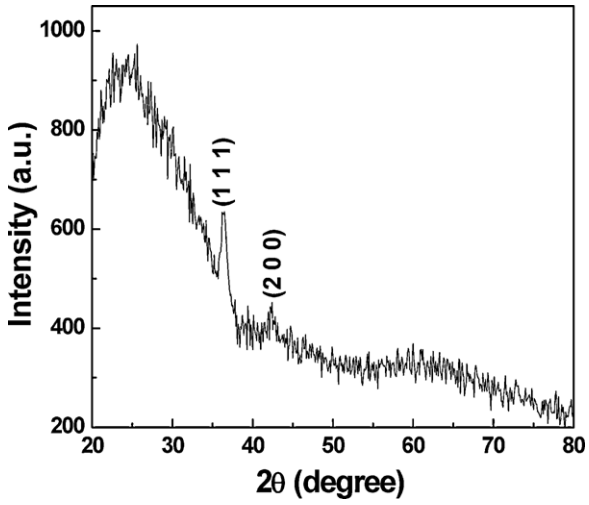

Fig. 2. X-ray diffraction pattern of as-deposited Cu_2O thin film onto glass substrate.

Fig. 2 shows the X-ray diffraction pattern of as-deposited Cu_2O thin film on to the amorphous glass substrate. The film exhibit the nanocrystalline nature with broad hump due to amorphous glass substrate. The short intense peaks at $2\theta = 36.48°$ ($d = 2.4635$ Å) and $2\theta = 42.19°$ ($d = 2.1335$ Å) corresponding to the (1 1 1) and (2 0 0) planes of Cu_2O with cubic crystal structure [18]. The crystallite size was estimated by using the well-known Scherrer's formula as,

$$D = \frac{0.9\lambda}{\beta \cos \theta} \quad (5)$$

where $\lambda = 1.5406$ Å for $CuK\alpha$, β is the full width at half maximum (FWHM) of the peak corrected for the instrumental broadening in radians and θ is the Bragg's angle. The sample of as-deposited Cu_2O thin film resulted in an average crystallite size of 11 nm.

The microstructure image of the Cu_2O thin film on glass substrate is as shown in Fig. 3(a). The as-deposited film shows micrometer size spherical grains (200–300 nm). These bigger size grains are formed due to agglomeration of small size nanoparticles. The film surface looks smooth and uniform. Appearance of small particles attaching to the surface of spherical grains are might be due to over growth observed with some content of small hydroxide phase having conductivity less than that of pure Cu_2O as seen by bright colour as compared to black spherical particles of pure Cu_2O.

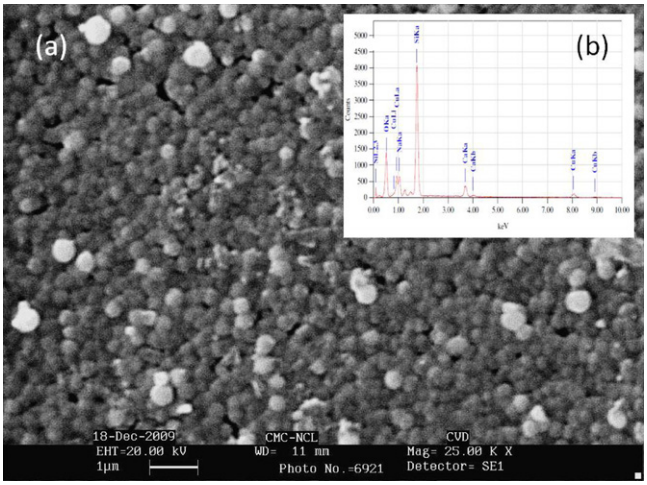

Fig. 3. (a) Scanning electron microscopy image, and (b) energy dispervive X-ray analysis spectrum of as-deposited Cu_2O thin film onto glass substrate.

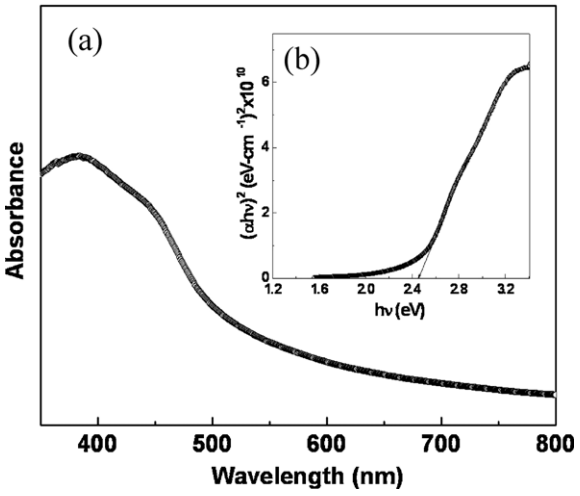

Fig. 4. (a) Plot of absorption vs. wavelength, and (b) variations of $(\alpha h\nu)^2$ vs. energy $(h\nu)$ of as-deposited Cu_2O thin film onto glass substrate.

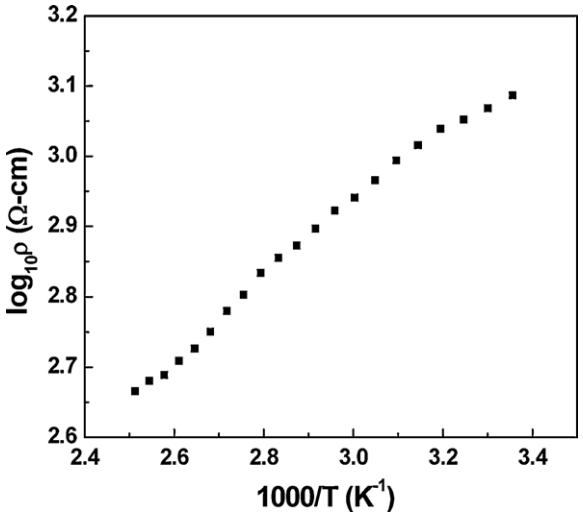

Fig. 5. Plot of log ρ vs. 1000/T for as-deposited Cu_2O thin film onto glass substrate.

Energy dispersive X-ray analysis (EDAX) spectroscopy measurement was used to determine the local composition of as-deposited Cu_2O thin film on the glass substrate. A typical EDAX spectrum is as shown in Fig. 3(b). The EDAX analysis shows the presence of copper (Cu), oxygen (O) and the presence of other elements like Na, Si and Ca is from the glass substrate. In the present case, small amount of surface contamination of oxygen cannot be excluded entirely and inclusion of hydrogen in hydroxyl phase cannot be detected by EDAX.

Fig. 4(a) shows the optical absorption spectra of Cu_2O film on the glass substrate in the wavelength range of 350–800 nm. The figure shows that absorbance decays exponentially with an increase in wavelength. The absorbance is large in the UV regions but decays very sharply within the UV–Vis boundary extending into the Vis region. The decay becomes relatively slower in the VIS and NIR regions. The nature of the transition (direct or indirect) is determined by using the relation

$$\alpha h\nu = A(h\nu - Eg)^n \quad (6)$$

where '$h\nu$' is the photon energy and 'Eg' the optical bandgap. 'A' is a constant which is related to the effective masses with the valence and conduction bands and n depends on the nature of the transition. For direct allowed transitions, $n = 1/2$ and for indirect allowed transitions, $n = 2$. Fig. 4(b) shows the plot of $(\alpha h\nu)^2$ vs. $h\nu$. The variation of $(\alpha h\nu)^2$ with $h\nu$ is linear which indicate that the direct allowed transition is present. The value of the optical band gap has been determined from the value of the intercept of the straight line at a $(\alpha h\nu)^2 = 0$. The as-deposited Cu_2O thin film shows the optical band gap 2.44 eV. In the literature Cu_2O thin film the reported band gaps are listed as 2.1 eV [13], 2.17 eV. [1], 2.20 eV [22], 2.25 eV [10] and 2.35 eV [19]. The band gap value is much greater that the reported which clearly demonstrate the enhancement in band gap due to decreasing particle size.

The two-point DC probe method was employed to understand the variation of electrical resistivity in the temperature range 300–400 K in air atmosphere. The room temperature electrical resistivity of as-deposited Cu_2O thin films on glass substrates was found to be 1.2 kΩ-cm which is quite lower than the reported value [20]. Fig. 5 shows a plot of inverse absolute temperature verses log (resistivity) for a cooling cycle. The dependence is almost linear indicating the presence of only one type of conduction mechanism in the film. Since, our experimental data fit into the relation,

$$\rho = \rho_0 \exp\frac{-Ea}{kT} \quad (7)$$

where ρ is the resistivity at temperature T, ρ_0 is a constant, k is Boltzman's constant, T is the absolute temperature and Ea is the activation energy. In this case, activation energy was calculated from linear portion of the graph and is found to be 0.105 eV. Although film preparation methods are different, these values are quite comparable with the reported one [21,22] for Cu_2O thin film. The decrease in resistivity with increase in temperature confirms the semiconducting behavior of the Cu_2O film.

In the thermo e.m.f. measurement, the temperature difference causes the transport of carriers from the hot end to the cold end and thus creates an electric field, which gives the thermal voltage. This thermally generated voltage is directly proportional to temperature difference created across the semiconductor. It was found that the polarity of thermally generated voltage at the cold end for Cu_2O thin film is positive indicating Cu_2O is p-type semiconductor.

5. Conclusions

Simple and inexpensive method, namely, chemical bath deposition (CBD), has been successfully used to synthesize nanocrystalline Cu_2O thin films on amorphous glass substrates. A dense, smooth and homogeneous film was observed by surface morphology. Bigger size grains were clearly observed due to agglomeration of smaller ones with the band gap value of 2.44 eV with a p-type electrical conductivity.

Acknowledgements

The authors are extremely grateful to Dr. A.S. Patil, Principal, P.S.G.V.P. Mandal's Arts, Commerce and Science College Shahada for his constant support to carry out this research work, Dr. N.O. Girase, Principal, S.V.S.'s Arts and Science College Dondaicha for his encouragement, support and fruitful discussions. The authors (PBA) and (RSP) acknowledge with gratitude the financial support from the University Grant Commission Pune.

References

[1] R.N. Briskman, Sol. Energy Mater. Sol. Cells 27 (1992) 361–368.
[2] C.A.N. Fernando, L.A.A. De Silva, R.M. Mehra, K. Takahashi, Semicond. Sci. Technol. 16 (2001) 433–439.
[3] X. Mathew, N.R. Mathew, P.J. Sebastian, Sol. Energy Mater. Sol. Cells 70 (2001) 277–286.
[4] Z.Z. Chen, E.W. Shi, Y. Zheng, W.J. Li, B. Xiao, J.Y. Zhuang, J. Cryst. Growth 249 (2003) 294–300.
[5] S.C. Ray, Sol. Energy Mater. Sol. Cells 68 (2001) 307–312.

[6] D.P. Singh, Jai Singh, P.R. Mishra, R.S. Tiwari, O.N. Srivastava, Bull. Matter. Sci. 31 (2008) 319–325.
[7] Y.S. Gong, C. Lee, C.K. Yang, J. Appl. Phys. 77 (1995) 5422–5425.
[8] M. Parhizkar, S. Singh, P.K. Nayak, N. Kumar, K.P. Muthe, S.K. Gupta, R.S. Srinivasa, S.S. Talwar, S. Major, Colloids Surf. A: Physicochem. Eng. Aspects 257–258 (2005) 277–282.
[9] A.A. Ogwu, T.H. Darma, E. Bouquerel, J. Achievements Mater. Manuf. Eng. 24 (2007) 172–177.
[10] M. Hari Prasad Reddy, P. Narayan Reddy, S. Uthanna, Indian J. Pure Appl. Phys. 48 (2010) 420–424.
[11] B. Balamurugan, B.R. Mehta, Thin Solid Films 396 (2001) 90–96.
[12] S. Szu, C.L. Cheng, Mater. Res. Bull. 43 (2008) 2687–2696.
[13] Y. Li, J. Liang, Z. Tao, J. Chen, Mater. Res. Bull. 43 (2008) 2380–2385.
[14] W. Shang, X. Shi, X. Zhang, C. Ma, C. Wang, Appl. Phys. A 87 (2007) 129–135.
[15] M.T.S. Nair, L. Guerrero, O.L. Arenas, P.K. Nair, Appl. Surf. Sci. 150 (1999) 143–151.
[16] J.M. Valtierra, S. Calixto, F. Ruiz, Thin Solid Films 460 (2004) 58–61.
[17] H.M. Pathan, C.D. Lokhande, Bull. Mater. Sci. 27 (2004) 85–111.
[18] ASTM data card file No.78-2076.
[19] T. Maruyama, Sol. Energy Mater. Sol. Cells 56 (1998) 85–92.
[20] T. Mahalingam, J.S.P. Chitra, S. Rajendran, P.J. Sebastian, Semicond. Sci. Technol. 17 (2002) 565–569.
[21] U.D. Lanke, M. Vedawyas, Nucl. Instrum. Method Phys. Res. B 155 (1999) 97–101.
[22] N. Serin, T. Serin, S. Horzum, Y. Celik, Semicond. Sci. Technol. 20 (2005) 398–401.